Received: 2 May 2019 | Revised: 13 February 2020 | Accepted: 2 March 2020
DOI: 10.1002/we.2499

WILEY

RESEARCH ARTICLE

Evaluation of PMSG-based drivetrain technologies for 10-MW floating offshore wind turbines: Pros and cons in a life cycle perspective

Farid K. Moghadam | Amir R. Nejad

Department of Marine Technology, Norwegian University of Science and Technology, Trondheim, Norway

Correspondence
Farid K. Moghadam, Department of Marine Technology, Norwegian University of Science and Technology, Trondheim, Norway.
Email: farid.k.moghadam@ntnu.no

Abstract

This paper presents an in depth evaluation and comparison of three different drivetrain choices based on permanent-magnet synchronous generator (PMSG) technology for 10-MW offshore wind turbines. The life cycle approach is suggested to evaluate the performance of the different under consideration drivetrain topologies. Furthermore, the design of the drivetrain is studied through optimized designs for the generator and gearbox. The proposed drivetrain analytical optimization approach supported by numerical simulations shows that application of gearbox in 10-MW offshore wind turbines can help to reduce weight, raw material cost, and size and simultaneously improve the efficiency. The possibility of resonance with the first torsional natural frequency of drivetrain for the different designed drivetrain systems, the influence of gear ratio, and the feasibility of the application for a spar floating platform are also discussed. This study gives evidence on how gearbox can mitigate the torque oscillation consequences on the other components and how the latter can influence the reliability of drivetrain.

KEYWORDS

drivetrain optimization, floating offshore wind turbine, life cycle assessment, permanent-magnet synchronous generator

1 | INTRODUCTION

The capacity of offshore wind turbines and the distance from shores is rising rapidly, so that multigigawatt offshore wind farms based on multimegawatt floating turbines show potentials to be one of the dominant sources of power production in the future. The latter is due to availability of better wind resources, less turbulence, steadier winds, and less wind shear; easier transportation of larger turbines on the sea; technological developments in power electronic converters and direct current (DC) power transmission technologies; the establishments of required market infrastructures; and technological achievements in installation of turbines in deep waters, which lead to a considerable drop in the levelized cost of energy (LCOE) of offshore wind turbines. In spite of significant improvements, there are still no unanimous decision about the drivetrain system technology in offshore wind turbines.[1,2] Offshore wind reaches to 10-MW turbines or even higher, but there are still different interests between manufacturers in the selection of drivetrain technology. One reason is that the drivetrain in wind originally comes from available experiences in other industries, which has been modified over time. The latter has then been upscaled for higher powers with some modifications to reduce the production costs and improve the dynamic response. Because the wind turbines are developed for a wide range of power in various onshore/offshore, fixed/floating, two-/three-bladed rotors, upwind/downwind, high/medium/low wind, fix/variable speed, stall/active yaw, and stall/active pitch applications, a customized design of the drivetrain for the cost reduction and performance improvement is inevitable. Therefore, there is a need for a special drivetrain design for each power class for different applications to have the lowest manufacturing, installation, and maintenance costs and simultaneously achieve the most reliable and efficient operation. The optimization of the drivetrain system also influences on the turbine design, because the size and weight of drivetrain is a main constraint in design of nacelle.

Even though the drivetrain system has an important share in manufacturing and maintenance of the turbine, and even if there are some researches conducted on the optimization of the components of the drivetrain, there is no analytical study about a system-level optimization of the drivetrain for 10-MW floating wind turbine applications as of the authors' knowledge. The proof for this claim is the different technology interests in offshore wind turbine industry. Because the drivetrain is a complex electromechanical system, the optimization of this system is a multidisciplinary task that calls for external system-level and internal component-level optimization problems. The other circumstance is that the optimizations need to be performed over the life cycle of the system, consisting of design, manufacturing and installation, and operation and maintenance (O&M). In this paper, different permanent magnet synchronous generator (PMSG)-based drivetrain technologies, that is, direct-drive permanent-magnet synchronous generator (DDPMSG), medium-speed permanent-magnet synchronous generator (MSPMSG), and high-speed permanent-magnet synchronous generator (HSPMSG), are designed and compared. This work is a starting point for the optimization of drivetrain systems for large offshore wind turbines from design, manufacturing, and O&M perspectives. It will be shown that a thoughtful selection of technology can considerably reduce the drivetrain weight and cost, while improving the overall efficiency and dynamic response. The numerical results show that the drivetrain system based on MSPMSG could be the most promising choice for 10-MW floating offshore wind turbines.

Four assumptions are made in this research:

1. There are some limitations such as availability of a technology, vendors, and raw materials that influence on companies' drivetrain selection. The latter will not be discussed in this research.
2. The purpose of analytical design of the drivetrain components is to provide input data for the comparison study between different drivetrain technologies. Complementary component-level detailed design steps such as finite element analysis for more detailed electromagnetic, structural, and thermal designs are not in the scope of this research.
3. Reliability calculations for under consideration drivetrain systems are not in the scope of this paper, but how the failure modes are affected by the drivetrain technology is discussed.
4. For each drivetrain technology, the conventional configuration is considered in this study. Some innovative wind turbine drivetrain systems, such as gearbox integrated main-bearing (used eg in Areva Multibrid M5000 medium-speed technology) and hub-supported drivetrain (used eg in GE Haliade 150-6MW direct-drive technology) based on more compact and lightweight designs, are not the focus of this work.

The study is carried out on the basis of the most conventional drivetrain configurations available in the market, and the results provide a baseline for any further investigations on 10-MW PMSG-based wind turbine drivetrain systems. The life cycle approach for performance assessment of the different drivetrain topologies based on the PMSG technology over the design lifetime is introduced. Over the life cycle, the research focus will be on design, manufacturing, and operation supported by an analytical model of the drivetrain components. On this basis, the contributions of this paper are the following:

1. Drivetrain performance assessment using the life cycle approach is introduced.
2. A new drivetrain optimization approach is proposed, which ensures an optimized overall cost and weight, improves the reliability and efficiency, and simultaneously assesses the feasibility of the design.
3. A new analytical design approach is proposed for the optimized design of PMSG based on the optimization of the active material cost. The optimization problem is solved numerically, and the global optimizer is determined. The design is validated by ANSYS-RMxprt software.
4. An analytical design model of the gearbox is presented, and a new optimization approach is proposed to optimize the gearbox weight. KISSsoft software is used to validate the feasibility of the design.
5. A comprehensive comparison between the design, raw material cost, weight, size, efficiency, and reliability of DDPMSG, MSPMSG, and HSPMSG drivetrain technologies is presented.
6. The first torsional natural frequency of three under consideration drivetrain technologies is calculated, and the feasibility of application in floating offshore wind turbines is investigated.

The selection of drivetrain technology is a multidisciplinary task that needs to compromise between the criteria obliged by the life cycle assessment approach. By using DDPMSG, the generator will be larger, heavier, and more expensive, which can also increase the weight and the cost of nacelle, tower, and platform consequently. The latter also affects the installation and maintenance costs. The first research problem would be if the extra weight of a low-speed generator could compensate the weight reduction due to the gearbox removal. The second question is if the elimination of gearbox can improve the reliability because the nullification of one of the subsystems in a serial system seems to help reach a higher reliability if the reliability of components is fixed. The third challenge is if the gearbox removal can improve the drivetrain efficiency using the same justification that was provided for the reliability. The last question is which topology can safely work with floating offshore platform, which is expected to be widely used in high-power offshore wind turbines. This research uses analytical models of the drivetrain components along with numerical optimization techniques and deals with the described research problems. It is analytically proven that for the under consideration range of speed and power, gearbox helps to improve the operation and reduce the raw material cost of drivetrain. The main focus of this work is studying about the design interactions and dynamic couplings between gearbox and generator in offshore floating wind turbines' drivetrain systems. Higher level details of the drivetrain design including the design of main bearings, high-speed and low-speed shafts, and bedplate are not discussed in this work. The weight of bedplate has an important role on the drivetrain overall weight. The bedplate sizing depends on a wide range of parameters including drivetrain technology, rotor weight, rotor overhang, main shaft dimension, main bearings weight, gearbox weight,

generator weight, converter weight, and transformer weight. In addition to individual component weights that the bedplate must support, the bedplate model must take into account rotor loads. For the design of bedplate for the under consideration drivetrain systems, readers are referred to Guo et al.[3,4]

The paper is organized as follows: The state-of-the-art of wind turbine drivetrain technologies for offshore and onshore applications is presented in Section 2. In Section 3, the drivetrain life cycle performance assessment approach and the proposed drivetrain optimization algorithm are described. The analytical design and optimization procedure of the three under consideration PMSGs, that is, DDPMSG, MSPMSG, and HSPMSG, and the associated gearboxes are elaborated in the same section. Numerical simulations to validate the optimized generators and gearboxes design and a detailed comparison study between the under consideration drivetrain systems concerning cost, weight, operation, and performance are presented in Section 4. The paper is concluded in Section 5.

2 | STATE-OF-THE-ART TECHNOLOGIES

A review on commercialized drivetrain system technologies of wind turbines with a power higher than 4 MW is performed in this section. The dominant drivetrain technologies for the under consideration power are DDPMSG, MSPMSG, direct-drive wound rotor synchronous generator (DDWRSG), medium-speed wound rotor synchronous generator (MSWRSG), high-speed doubly fed induction generator (HSDFIG), and high-speed squirrel cage induction generator (HSSCIG) (Table 1). DDPMSG is the dominant technology of Siemens Gamesa (power range 6-8 MW) and GE (power range 6-12 MW) for fixed/floating platforms. MSPMSG is MHI Vestas' solution for the power higher than 8 MW, Aeorodyn for 6 MW, and Adwen and Areva for 8 and 5 MW, respectively. MSWRSG is Aerodyn's alternative for 8 MW. HSSCIG is the technology used by both Siemens and Vestas (power range 3-4 MW). HSDFIG is the technology used by Senvion and REpower for 6.2 MW offshore. DDWRSG is the Enercon technology interest for the power up to 8 MW but for onshore applications. Some research-scale offshore drivetrain designs prototyping in the 5 to 12 MW range have also been considered in this study. An overview of the most recent application of different drivetrain technologies is shown in Table 2. Based on this summary, all these technologies show potentials for the drivetrain in offshore wind turbines. Even though the most recent literature recommends DDPMSG because of efficiency and reliability considerations,[5] the diversity in drivetrain technology interests in both industry and academia shows that other factors influence on the selection of the wind turbine drivetrain. In the meantime, there are many other technologies that have not been commercialized. For instance, direct-drive and medium-speed DFIG with a high number of poles are less efficient due to a high excitation loss.[6] Brushless DFIG is not an efficient machine due to a low-power torque density compared with typical induction and synchronous generators.[7] Superconducting direct-drive synchronous generators are still far from being commercialized regarding standardization and some open paths to explore regarding cost and reliability.[8] An overview on the commercialized turbines (see Table 2) and the reference turbines developed by research institutions and universities[9,10] shows a unanimous interest in PMSG for high-power offshore wind turbine drivetrain systems. Higher efficiency due to external excitation circuit removal, higher reliability and availability, and less maintenance costs due to the compactness and lightweight design and brushes elimination are the motivations.[10] Different designs for permanent-magnet generators are proposed in the literature. The latter includes vernier/conventional generators, axial/radial flux, surface-mounted/interior rotor magnets, slotted/slotless stator, inner/outer rotor, distributed/concentrated winding, and integer-/fractional-slot winding machines.[11] However, still, the commercialized designs for wind turbine drivetrain systems, that is, radial flux, inner rotor, and surface-mounted PMSGs, are the focus of this research.

In the continued section, the priorities which may be considered by the different turbine manufacturers in selection of the PMSG drivetrain technology is analytically studied. It is aimed to find which PMSG-based drivetrain topology will probably be the future trend based on the analysis of the available choices. The power range and turbine platform are emphasized as the other important criteria which affect the drivetrain technology chosen by different manufacturers.

3 | METHODOLOGY

For this study, the DTU 10 MW reference wind turbine is used.[9] The parameters of the DTU turbine used for the drivetrain studies are listed in Table 3. The other parameters related to the drivetrain components are updated based on the designed generators and gearboxes in this paper.

3.1 | Life cycle approach

In the life cycle performance assessment approach, to have a meaningful comparison between different drivetrain technologies, the overall costs and benefits are evaluated over the design lifetime, and the outcome is expressed by using levelized values as equivalent costs and benefits at the regular intervals during all the system life. By using this method, the costs and revenues of various drivetrain technologies are needed to be studied over design, manufacturing, installation, O&M, life extension, and decommissioning[12] (see Figure 1). The optimal configuration is the one that gives the highest profit over the cycle.

In design, concerns related to design, for example, complexities in design, maximal design utilization, and higher degree of adaptation to site-specific conditions, reliability, and controllability, are important. A preliminary failure modes study about the generator and gearbox in PMSG drivetrain is summarized in Table 4. It is interesting to observe that the most of failure modes can be rooted back to design stage. In

TABLE 1 State-of-the-art of drivetrain technologies in multimegawatt onshore and offshore wind turbines at a glance (up to 10 MW)

Technology	Layout
1. High-speed squirrel cage induction generator • Merits: cheap, simple generator design • Drawbacks: sensitive to transients, low efficiency	
2. High-speed doubly fed induction generator • Merits: cheap, fractional converter • Drawbacks: sensitive to transients, low efficiency	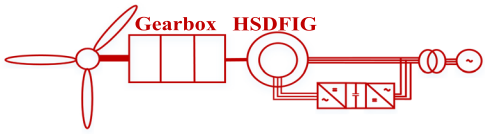
3. Direct-drive wound rotor synchronous generator • Merits: cheap • Drawbacks: brushes, low efficiency, higher weight	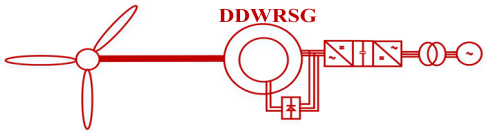
4. Medium-speed wound rotor synchronous generator • Merits: cheap • Drawbacks: brushes, low efficiency	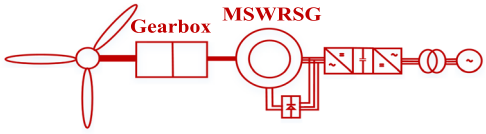
5. Direct-drive permanent-magnet synchronous generator • Merits: low maintenance, high efficiency • Drawbacks: expensive	
6. Medium-speed permanent-magnet synchronous generator • Merits: low maintenance, high efficiency, less weight for higher powers • Drawbacks: expensive	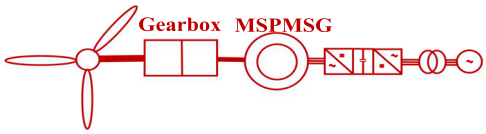

reliability-based design, one should look at the reliability of a drivetrain design considering failure modes to ensure a safe and reliable operation over the operating speed and torque range. However, the failure modes depend on the drivetrain technology. Furthermore, regarding specific operating conditions, some modes are of a higher importance. The failure functions will then be defined for the components and subsequently the drivetrain system based on a criticality analysis of the failure modes of the components. The impacts of uncertainty sources such as wind, wave, material strength model, and power grid can be modelled by using safety factors in a deterministic design or applying a multiplicative model of uncertainties in a stochastic design approach.[18] The outcome of reliability-based design will specify the expected lifetime of drivetrain system. For new systems and applications, for example, PMSG-based drivetrain systems for 10 MW spar floating offshore wind turbine, due to the lack of standards for the design load cases, design is more challenging, which requires to leverage the similar experiences accompanied by a wide range of numerical simulations. As a design study in this paper, the first torsional natural frequency of under consideration PMSG-based drivetrain systems is studied, and design remarks are given about the feasibility of using these technologies in floating platforms.

In manufacturing and installation, weight, compactness, and special manufacturing and installation requirements should be taken into consideration. An example of more manufacturing efforts is in manufacturing DDPMSG, where the too high pole count causes small rotor poles with fine stator slotting, which makes manufacturing expensive. About installation efforts, for instance, less weight drivetrain technology and the consequent reduced weight nacelle and tower help to reach less cost transportation and craning requirements. For more clarification, a promising solution for a floating wind turbine transport and installation is to preassemble the whole turbine in one piece in the shipyard, towing to the

TABLE 2 Drivetrain most conventional technologies

HSSCIG	HSDFIG	DDWRSG	MSWRSG	DDPMSG	MSPMSG
SWT-4.0-130	GE 5.3-153	EN136-4.2	SCD 8.0/168	SG 8.0-167 DD	V164-10.0MW
Siemens	General Electric	Envision	Aerodyn	Siemens	Vestas
4 MW	5.3 MW	4.2 MW	8 MW	8 MW	10 MW
Offshore/onshore	Onshore	Offshore/onshore	Offshore	Offshore	Offshore
Geared (1:119)	Geared (NA)	Direct-drive	Geared (1:27)	Direct-drive	Geared (1:38)
V136-4.2 MW	6.2M126	E-126 7.580	NA	YZ150/10.0	Adwen AD 8-180
Vestas	Senvion	Enercon	NA	Swiss Electric	Adwen
4 MW	6.2 MW	7.6 MW	NA	10 MW	8 MW
Onshore	Offshore	Onshore	NA	Offshore	Offshore
Geared (NA)	Geared (1:97)	Direct-drive	NA	Direct-drive	Geared (1:41)

Abbreviations: DDPMSG, direct-drive permanent-magnet synchronous generator; DDWRSG,direct-drive wound rotor synchronous generator; HSDFIG, high-speed doubly fed induction generator; HSSCIG, high-speed squirrel cage induction generator; MSPMSG,medium-speed permanent-magnet synchronous generator; MSWRSG, medium-speed wound rotor synchronous generator.

TABLE 3 Turbine specification[9]

Parameter	Value
Rated power (MW)	10
Rated rotor speed (rpm)	9.6
Rated wind speed (m/s)	11.4
Equivalent driveshaft linear spring constant (N.m/rad)	2,452,936,425
Rotor moment of inertia J_r $(kg.m^2)$	8×10^8

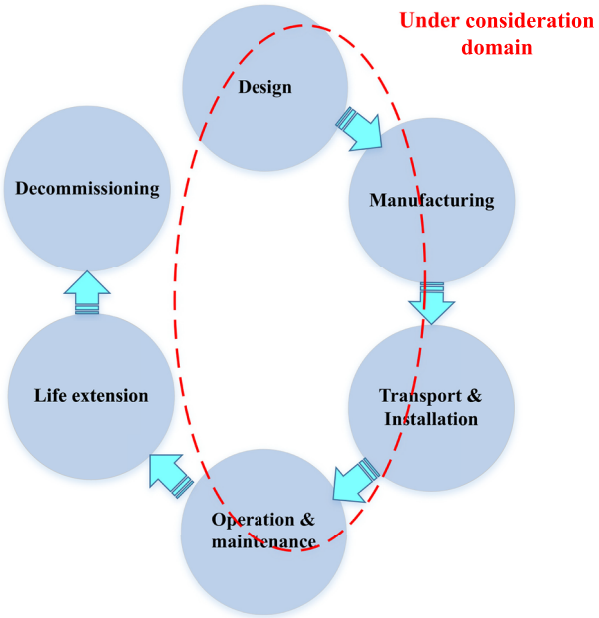

FIGURE 1 Drivetrain life cycle assessment approach [Colour figure can be viewed at wileyonlinelibrary.com]

offshore deployment site, and using a large floating crane to hook up with mooring systems,[19] where the most important limitation is the turbine weight. A significant part of this paper is dedicated to the optimization of weight, raw material cost, and size for under consideration drivetrain technologies as a necessary input to study manufacturing and installation costs.

In O&M, performance, efficiency, reliability, availability, and maintenance costs are required to be addressed. In offshore wind turbine applications, especially in high-power floating installations in deep waters, due to farther distance from shores, broader ranges of excitation sources and motions, and utilization of large, massive, and expensive components, any improvement in efficiency, reliability, and availability can help to reduce cost of electricity. It is reported that O&M contributes in order of 30% of LCOE in offshore wind turbines.[20] In *performance*, the quality of generator output power is concentrated, where the generator technology and the power frequency converter play a significant role. In *efficiency*, improving the efficiency of the drivetrain is discussed. It is needed to evaluate which technology and configuration will give a greater efficiency, which helps to reduce the electricity cost. Therefore, there will be a need to look into all the individual components of the drivetrain system. Then, the overall efficiency in the rated power is calculated/compared for the different technologies. In *reliability*, the failure rates of different drivetrain components and fault tolerance properties of each technology is required to be analyzed. Therefore, the failure modes of the subcomponents must be listed, so that the components and subsequently the drivetrain systems could be studied/sorted according to the

TABLE 4 Basic failure modes study of PMSG drivetrain components

PMSG[11,13-15]	Gearbox[16,17]
Possible faults	**Possible faults**
Mechanical faults	*Gear fault*
Blocking bearings	*Shaft fault*
Stucking filings in the air gap	*Bearing fault*
Electrical faults	Shaft misalignment
Short circuit faults	Shaft bending
Finite resistance circuit faults	Shaft loose
Open circuit faults	*Housing fault*
Magnetic faults	*Fastener fault*
Demagnetization of rotor magnets	*Seal fault*
Detachment of rotor magnets	**Fault reasons**
Fault reasons	Underestimated design loads
Overcurrent	Torque overloads
Voltage sags, swells, and harmonics	Material defects
Cooling and lubrication system maloperation	Manufacturing errors
Sensors and communication network maloperation	Dirt in the lubricant or poor lubrication
Rotor torque oscillation by wave-/wind-induced moments	Damage during transportation and assembly
Electromagnetic torque oscillations	Misalignment of components in the shaft
Poor or contaminated bearing lubrication	**Failure modes**
Bearing installation problems	Gear wear; scuffing and contact fatigue (fatigue)
Failure modes	Gear plastic deform; crack; fracture; bending (ultimate = fatigue)
Stator winding insulation fail (fatigue, ultimate)	Bearing spalling : excessive load = poor lubrication (fatigue)
Demagnetization: magnet heating (ultimate)	Bear: smearing : foreign objects trapped within (fatigue)
Demagnetization: increased flux density (ultimate)	Bear: worn surface : skewed roller = lubrication (fatigue)
Phase/path cutoff (fatigue, ultimate)	Bear: partial chipping of rings = roller : excessive load (fatigue)
Stator tooth fretting damage/crack (fatigue/ultimate)	Bear: ring split = crack : excessive load = loose fit (fatigue)
Detached magnet: raised centrifugal forces (fatigue)	Bear: fretting corrosion : fluctuating load = lubrication (fatigue)
Bearing pitting and sanding (fatigue)	Bear: electrical pitting : sparks by electric current (fatigue)
Bearing brinelling/false brinelling (fatigue)	Bear: damaged retainer : heavy vibration = speed change (fatigue) different

Abbreviation: PMSG, permanent-magnet synchronous generator.

highest to the lowest probability of failure regarding the most critical failure modes. The latter can be based on the failure reports if enough event logs and trouble shooting reports of the operation are available. It can also be based on the post processing of real operational data measured from the system[21] to calculate the fatigue damage and remaining useful life of the system. The latter could be supported by sufficient simulated models under the different load cases dependent on the application. In general, a combination of these two approaches is used. Obtaining the vulnerability map for each component considering the critical failure modes, which indicates the subcomponents from the highest to lowest probability of damage is the basis for reliability-based maintenance. The latter supported by lifetime-predicting models will give an insight about the reliability and remaining lifetime of the system, which is needed to be done for the different drivetrain technologies. In *availability*, the downtimes of the wind turbine due to the drivetrain shutdowns, including downtimes for periodic maintenance or unscheduled repairs for different technologies, are needed to be discussed. Furthermore, the possibility of using modular design for different gearboxes and generators for reduction of downtime in different drivetrain technologies relates to availability studies. In order to compare reliability and availability of different technologies, a detailed analysis of each component's failure modes, probability of failure, and the downtimes is required. Maintenance costs will relate to the failure rate of components, labor, parts, operations, equipment, and facilities.[22] The technology of high-power floating offshore wind turbines is new, and there are only few operational turbines of this type. An accurate O&M comparison between different technologies relies on an access to operational data of the same system under the same load cases; however, approximated analyses can be attained based on available experiences in lower power ranges, similar experiences from other industries, some limited data in access from the same operational turbines and applications, scaled-down laboratory-based systems, supported by high-fidelity simulation models and theoretical analyses. Each drivetrain technology is finally needed to be scored based on O&M criteria, namely, efficiency, reliability, availability, and maintenance costs. The other fact that makes O&M analysis more difficult is that each drivetrain technology is a different dynamic system with different responses. To maintain the tip speed ratio of larger rotors in higher powers to reach the highest power coefficient, the nominal rotational speed of rotor is reduced, which causes different dynamic responses even for the turbines of the same technology but a different rated power. Moreover, floating offshore platforms encounter turbines into different motions induced by the synergistic impacts of wind and wave, the gravity of the turbine, and the floating platform. The lower rotor speed and more diverse and higher amplitude excitations necessitate a special O&M study for the drivetrain in high-power floating applications. In this research, for the under consideration PMSG-based drivetrain topologies, the overall efficiency is calculated/compared considering the efficiency of the individual components. As a reliability analysis, the drivetrain failure modes affected by the rotor torque and generator electromagnetic torque oscillations of different technologies are discussed and compared. Unequal

TABLE 5 Case study technologies

Technology	Type 1 (DDPMSG)	Type 2 (MSPMSG)	Type 3 (HSPMSG)
Rated power(MW)	10	10	10
Application	Floating offshore	Floating offshore	Floating offshore
Generator	PMSG	PMSG	PMSG
Gearbox	Direct-drive	Three stages (1:50)	Three stages (1:156)

Abbreviations: DDPMSG, direct-drive permanent-magnet synchronous generator; HSPMSG, high-speed permanent-magnet synchronous generator; MSPMSG, medium-speed permanent-magnet synchronous generator; PMSG, permanent-magnet synchronous generator.

cogging torque values in different drivetrain technologies cause different rotational vibration performances. The part of the life cycle that is emphasized is specified in Figure 1.

3.2 | Proposed drivetrain design optimization

The selection of drivetrain technology is a multidisciplinary task that needs to make compromises between the criteria obliged by the life cycle approach. As explained earlier, PMSG is the promising technology for high-power offshore wind turbines. Because 10 MW PMSG-based drivetrain can be realized by different gear ratios, it is needed to assess different gear ratios over the life cycle. Gear ratio as per definition in IEC 61400-4 is $\frac{n}{n_r}$, where n and n_r are the speeds of input and output shafts, respectively.[23] The three under consideration drivetrain topologies are DDPMSG, MSPMSG, and HSPMSG technologies, which are specified in Table 5). The 2D view of PMSG overall design that is used for the three under consideration drivetrain technologies is shown in Figure 2A. DDPMSG is a direct-drive technology. MSPMSG is the medium-speed drivetrain technology, which can be realized by either two or three stages. The operational high-power medium-speed technologies are often based on hybrid gearboxes containing three stages, including planetary gears in the upwind stages and parallel gear pairs, which can be used to realize the gear ratio 1 : 36 to 1 : 108. The mentioned gearbox topology is selected for the MSPMSG drivetrain technology in the paper. HSPMSG is a high-speed drivetrain technology. The gearbox for the high-speed technology can be realized by three planetary stages with a gear ratio variable from 1 : 108 to 1 : 216. The gearbox topology for the MSPMSG and HSPMSG drivetrain technologies is shown in Figures 2B and 2C. In industry, based on the rule of thumb, the conventional parallel stage is used for realization of the inverse of gear ratio $1 < \alpha < 3$, and a conventional planetary stage is used for $3 < \alpha < 6$. For $1 < \alpha < 3$, the industry interest is in using a parallel stage. The reason that planetary gear is not dominant for $1 < \alpha < 3$ is due to more complex design and manufacturing, more difficult access for maintenance, and difficulty in fault detection and condition monitoring. Therefore, for the realization of the gear ratio 1 : 50 suggested in DTU 10-MW turbine design, the gearbox topology based on two planetary gear stages and one parallel stage is studied in the paper as the most conventional topology to realize the similar gear ratios in the medium-speed wind turbine drivetrain systems but for lower power ranges. In the power range 10 MW in a medium-speed application, there is no agreed topology and gear ratio in the gearbox design. Some manufacturers have recently used other design topologies to meet better the requirements of offshore application by a less weight and more robust design under load variations, for example, Vestas V164-9.5MW and Adwen AD 8MW-180 have used three-stage compound planetary stages and two-stage compound planetary stages, respectively, to realized the gear-ratios 1 : 38 and 1 : 41. Because no reference was found, which prohibits the utilization of three planetary stages to realize an MS gearbox, another MS topology based on three planetaries is also studied. For the HS design with the assumed gear ratio 156, the most practical way to realize the gearbox is using three planetary stages.

Larger generator in DDPMSG technology causes more costly manufacturing, installation, and maintenance. Even though the general idea is that a direct-drive generator is more reliable, available, and efficient due to a gearbox removal (eg, in Polinder et al[20,25] and Zhang et al[24]), the different generators and gearboxes in DDPMSG, MSPMSG, and HSPMSG drivetrain technologies result in different dynamic responses, efficiencies, and weights of the components and the drivetrain, which calls for an analytical study before judging about operations and economics. Generator and gearbox are focused. The other significant components are converter system and main bearings. The main bearings in the under consideration technologies are the same because they are placed on low-speed side. The power converter system depends on rated power and voltage. Because the three generators are designed for the same power factor and consequently apparent power, the rated power of the converters is the same. However, the increased design voltage in MSPMSG and HSPMSG drivetrains compared with DDPMSG helps to reach a higher efficiency for the power converter with less effort due to reduction of switching losses, but the increased voltage raises the power converter cost due to the increased cost of the switches, DC link, and some auxiliary circuits. The changes in the overall drivetrain efficiency and cost due to power converter are neglected.

The algorithm of the proposed PMSG drivetrains evaluation is demonstrated by the flowchart in Figure 3. From the conceptual design perspective, the gearbox affects both the input torque and speed of the generator. The latter are among the critical parameters in design of generator so that the size of generator is directly proportional to these parameters. In each iteration of the proposed drivetrain optimization approach, the gear ratio is fixed by the outer loop. Therefore, the optimization problem of each drivetrain technology is broken into two decoupled problems of gearbox and generator optimizations. As a result, for each drivetrain topology, two internal component-level optimization problems are solved. The first problem looks for the optimized design of the generator. The generator optimization problem is designed to ensure the minimization of cost of active material while maximizing the generator torque density. The second problem is a cost (weight) optimization of the

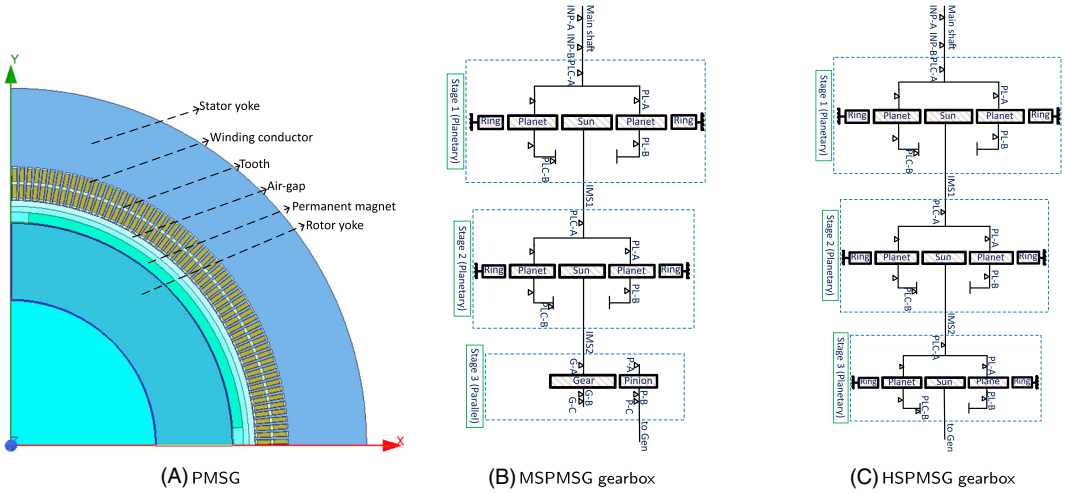

(A) PMSG (B) MSPMSG gearbox (C) HSPMSG gearbox

FIGURE 2 Topology of generator and gearbox in this study. HSPMSG, high-speed permanent-magnet synchronous generator; MSPMSG, medium-speed permanent-magnet synchronous generator; PMSG, permanent-magnet synchronous generator [Colour figure can be viewed at wileyonlinelibrary.com]

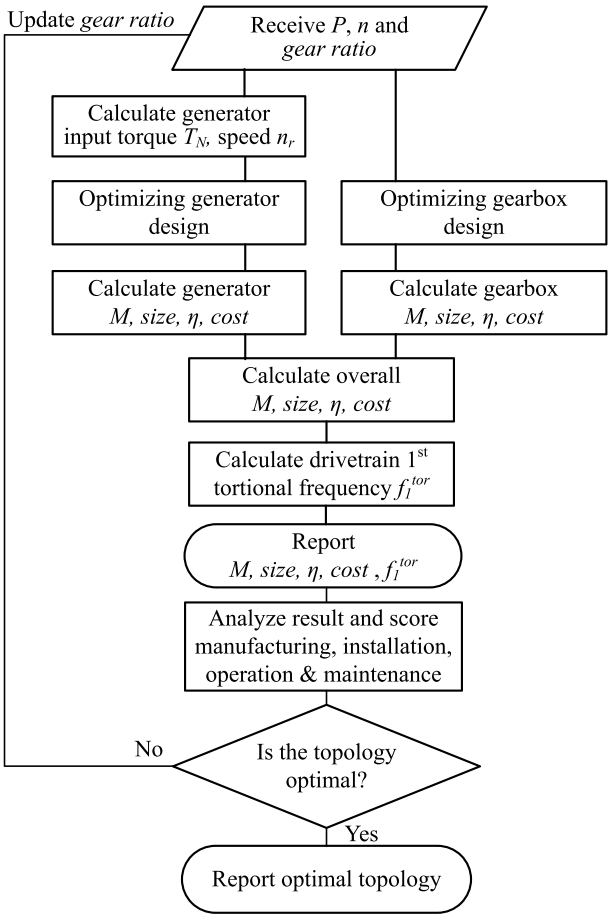

FIGURE 3 Proposed drivetrain optimization approach

multistage gearbox. Drivetrain performance-based and reliability-oriented constraints are imposed to the component-level optimization problems to ensure the feasibility of the generator and gearbox proposed designs and a fair comparison between the under consideration drivetrain technologies. Finally, the designed drivetrain systems are compared with respect to total weight, cost, size, efficiency, and dynamic responses.

3.2.1 | Generator optimization

As discussed in Section 2, PMSG is the dominant technology for high-power offshore wind turbines. Some motivations are as follows:

1. Armature reaction is smaller in a permanent-magnet generator with surface-mounted magnets than in electrically excited generators, due to a larger air gap;

2. Losses of the field winding in electrically excited generators cause lower efficiency in these generators compared with permanent-magnet generators;
3. Besides reducing losses, the permanent-magnet generators lead to a lighter design. For the same power and frequency, compared with an electrically excited generator, a permanent-magnet generator can be realized with a smaller diameter, which is really helpful for design of high-power direct-drive generators for wind turbines[26]; and
4. It is believed that permanent-magnet generators are more reliable than electrically excited generators. One reason is that excitation circuits, the associated power electronics semiconductor devices, and the commutation rings and brushes cause a high portion of failures and downtimes in electrically excited generators, while they are not needed for permanent-magnet generators. The possible faults regarding the application of magnets, including magnets demagnetization and detachment can, to a great extent, be avoided by a proper design approach.

A three-phase radial flux, inner rotor, surface-mounted, slotted machine with laminated stator/rotor cores and distributed winding is the reference generator technology studied in this section. Reluctance torque, which is an important source of torque pulsations, is negligible in surface-mounted PMSGs. Low weight, simple design, and low-armature reaction are some other benefits of surface-mounted technologies.

Different objective functions with different sets of optimization variables are suggested in the literature for optimized design of PMSGs. Li et al[27] suggests the cost of the active material, Dubois et al[28] recommends the ratio of the cost of active material to torque density, and Røkke et al[11] proposes the cost of the active materials including the housing and the cost of the energy lost in the machine over its lifetime to be used to optimize the PMSG design.

In the continued part, an analytical design based on the minimization of the ratio of cost of active material to torque density is used to find the optimized design of the generator in DDPMSG, MSPMSG, and HSPMSG technologies. The latter ensures the minimum cost while maximizing the electromagnetic (developed) torque density and utilization of the generator weight. The proposed analytical model represents the cost function and the design constraints as a function of five geometrical variables. The design procedure for the three under consideration generators is the same, but the parameters and constraints are adapted based on the operating voltage and speed.

The cost function C of the generator optimization problem is defined as

$$C_{\text{generator}}(\boldsymbol{x}) = \arg\min_{\boldsymbol{x}} \left(\frac{\text{cost}_{\text{active}}(\boldsymbol{x})}{T_d(\boldsymbol{x})} \right), \tag{1a}$$

$$cost_{active}(\boldsymbol{x}) = cost_{fe}(\boldsymbol{x}) + cost_{cu}(\boldsymbol{x}) + cost_{pm}(\boldsymbol{x}), \tag{1b}$$

$$T_d(\boldsymbol{x}) = \frac{T_N}{V(\boldsymbol{x})}, \tag{1c}$$

where x is a vector that represents the optimization variables. $cost_{active}$ is the cost of active materials in generator construction in Euro. The cost of active materials consists of the cost of iron used in rotor and stator yokes and stator teeth, copper of the stator windings, and the surface-mounted permanent magnets. $cost_{fe}$ is the total cost of iron, $cost_{cu}$ is the cost of copper, and $cost_{magnet}$ is the cost of magnet material. T_N is the nominal torque in $kN.m$, and V is the generator active volume in m^3. T_d is the generator torque density in $kN.m/m^3$. The variables in Equation (1) are defined by

$$\boldsymbol{x} = [x_1, x_2, x_3, x_4, x_5]^T = [D_s, L_s, b_s, h_s, h_m]^T, \tag{2a}$$

$$cost_{cu} = c_{cu} m_{cu}, \tag{2b}$$

$$cost_{pm} = c_{pm} m_{pm}, \tag{2c}$$

$$cost_{fe} = c_{fe} m_{fe}, \tag{2d}$$

$$V = \pi \frac{D_{so}^2}{4} L_e, \tag{2e}$$

where the five optimization variables D_s, L_s, b_s, h_s, and h_m are the air gap diameter, active length of generator, slot width, slot height, and magnet height, respectively. c_{fe}, m_{fe}, c_{cu}, m_{cu}, c_{pm}, and m_{pm} are the specific costs and total weights of core, copper, and magnet, respectively. The design of surface-mounted PMSG deals with the determination of a high number of variables related to the generator geometry and operation. In the proposed optimized design approach, it was observed that all the generator design variables can be either defined as a function of the five geometrical optimization variables, or considered constant, or can change in optimization problem outer loops. The latter helped to turn a nonlinear and strongly nonconvex problem to a convex problem to be able to find a global optimizer. The other generator design variables, which are not assumed as a optimization variable, are classified into three different groups: first, those that can be written as a function of the five optimization variables, such as flux densities in air gap and teeth; second, the design variables that are assumed constant, for example, air gap thickness, which is fixed at the minimum value regarding the mechanical construction considerations of large permanent-magnet generators, and maximum flux densities in rotor and stator yokes; third, those variables that are updated/changed in outer loops to find their optimal values, for example, magnetic pole embrace $\left(\frac{b_m}{\tau_p}\right)$ and number of slots per pole and phase (q), but in each internal optimization take constant values. The

definition of m_{cu} in terms of the five optimization variables $(x_1, \ldots, x_5)$ is given in Equation (3a). The role of winding overhang, the slot wedge, and the insulation thickness is considered in the model. The weight of copper is proportional to the length and the cross section of the winding. The length is dependent on the generator length, the pole pitch, and the overhang, which is proportional to the voltage. The definition of m_{pm} in terms of the optimization variables is given in Equation (3b). $b_m\tau_p$ in this equation models the ratio of the pole surface that is covered by the magnet material to the all pole surface, which could take different values by using an optimization outer loop. The definition of the three components of m_{fe}, which respectively model the iron used for stator teeth, stator yoke, and the rotor core in terms of the optimization variables, is given in Equation (3c). The other variables in this equation are either constant or change by using external optimization loops. V in Equation (3d) is the overall volume of the generator, which is a function of generator equivalent length L_e and the stator outer diameter D_{so}. The generator equivalent length is a function of core length and air gap. The stator outer diameter is also a function of D_s, h_s, and stator yoke height h_{sy}. In Equation (3d), V is written in terms of the optimization variables.

$$m_{cu}(\boldsymbol{x}) = N\left(2x_2 + 2.5\left(\frac{\pi x_1}{p}\right) + 0.05\left(\frac{V_{ph}}{1000}\right) + 0.150\right)\left((x_3 - 2h_i)\frac{x_4 - h_w - 4h_i}{Q}\right)\rho_{cu}, \tag{3a}$$

$$m_{pm}(\boldsymbol{x}) = p\left(\frac{b_m}{\tau_p}\frac{\pi x_1}{p}\right)x_2 x_5 \rho_{pm}, \tag{3b}$$

$$m_{fe}(\boldsymbol{x}) = Q\left(\frac{\pi x_1}{Q} - x_3\right)x_4 x_2 \rho_{fe} + \tag{3c}$$

$$\pi\left(x_1 + 2x_4 + \frac{B_r x_5}{\frac{\mu_{pm}\pi x_1}{Q\left(\frac{\pi x_1}{Q} - \frac{x_3^2}{5(\delta + \frac{x_5}{\mu_{pm}}) + x_3}\right)}\left(\delta + \frac{x_5}{\mu_{pm}}\right)}\frac{4}{\pi}\sin\left(\frac{\pi b_m}{2\tau_p}\right)\frac{b_m}{\tau_p}\frac{\pi x_1}{p}\frac{x_2 + 2\delta}{2k_{fe}\hat{B}_{sy}x_2}\right)$$
$$\times \frac{B_r x_5}{\frac{\mu_{pm}\pi x_1}{Q\left(\frac{\pi x_1}{Q} - \frac{x_3^2}{5(\delta + \frac{x_5}{\mu_{pm}}) + x_3}\right)}\left(\delta + \frac{x_5}{\mu_{pm}}\right)}\frac{4}{\pi}\sin\left(\frac{\pi b_m}{2\tau_p}\right)\frac{b_m}{\tau_p}\frac{\pi x_1}{p}\frac{x_2 + 2\delta}{2k_{fe}\hat{B}_{sy}x_2}x_2\rho_{fe}$$
$$+ \pi\left(x_1 - 2\delta - 2x_5 - \frac{B_r x_5}{\frac{\mu_{pm}\pi x_1}{Q\left(\frac{\pi x_1}{Q} - \frac{x_3^2}{5(\delta + \frac{x_5}{\mu_{pm}}) + x_3}\right)}\left(\delta + \frac{x_5}{\mu_{pm}}\right)}\frac{4}{\pi}\sin\left(\frac{\pi b_m}{2\tau_p}\right)\frac{b_m}{\tau_p}\frac{\pi x_1}{p}\frac{x_2 + 2\delta}{2k_{fe}\hat{B}_{ry}x_2}\right)$$
$$\times \frac{B_r x_5}{\frac{\mu_{pm}\pi x_1}{Q\left(\frac{\pi x_1}{Q} - \frac{x_3^2}{5\left(\delta + \frac{x_5}{\mu_{pm}}\right) + x_3}\right)}\left(\delta + \frac{x_5}{\mu_{pm}}\right)}\frac{4}{\pi}\sin\left(\frac{\pi b_m}{2\tau_p}\right)\frac{b_m}{\tau_p}\frac{\pi x_1}{p}\frac{x_2 + 2\delta}{2k_{fe}\hat{B}_{ry}x_2}x_2\rho_{fe},$$

$$V(\boldsymbol{x}) = \frac{\pi}{4}\left(x_1 + 2x_4 + 2\left(\frac{B_r x_5}{\frac{\mu_{pm}\pi x_1}{Q\left(\frac{\pi x_1}{Q} - \frac{x_3^2}{5(\delta + \frac{x_5}{\mu_{pm}}) + x_3}\right)}\left(\delta + \frac{x_5}{\mu_{pm}}\right)}\frac{4}{\pi}\sin\left(\frac{\pi b_m}{2\tau_p}\right)\frac{b_m}{\tau_p}\frac{\pi x_1}{p}\frac{x_2 + 2\delta}{2k_{fe}\hat{B}_{sy}x_2}\right)\right)^2 \tag{3d}$$
$$\times (x_2 + 2\delta).$$

The definition of the variables used in the the above equations is given in Table 6. For more details on the design variables and their dependencies with the defined optimization variables, readers are referred to Grauers et al.[26] The results of the described optimization problem provide the detailed geometry, material consumption, cost, and the operational criteria such as efficiency, decoupled generator losses, power factor, flux densities, electrical and thermal loadings, induced and terminal voltages, and torque oscillations. The generator optimization problem including the objective function and the constraints is highly nonlinear. Because the resultant is a constrained nonlinear multivariable nonconvex problem in terms of the optimization variables, convex programming tools cannot be useful. Because the constraints are of a high number and mostly nonlinear, duality theories and associated dual problems add to the complexity of optimization. Problem reduction, using linear optimization,[11] and application of heuristic approaches, for example, genetic algorithm[27] are some alternatives suggested in the literature. Our observations show that the aforedescribed disciplined nonconvex problem shows a convex shape in a multidimensional graphical illustration of the objective function and constraints in the predefined range of optimization variables so that the problem is convex on a portion of its domain that is the feasible region regarding the constraints. Therefore, a global optimizer for this optimization problem could be found. MATLAB *fmincon* numerical optimization solver using sequential quadratic programming (SQP) algorithm is used to find the globally optimized design.

The objective function C is optimized subject to a wide range of specific electrical loading, magnetic loading, insulation and mechanical forces mitigation requirements, current density, armature thermal loading, power factor, and efficiency-based constraints to ensure a feasible design for the three generators. The carter factor is modelled in terms of the design variables in the optimization problems. The generators are assumed

TABLE 6 Generator optimization results

Generator Specifications	DDPMSG	MSPMSG	HSPMSG
Technical specification			
Number of poles p	200	12	4
Rated output power P_e (Mw)	10.003	10.004	10.000
Rated input torque T_N (MN.m)	10.689	0.202	0.065
Rated rotational speed n_r (rpm)	9.6	480	1497.6
Rated RMS line voltage V_L (kV)	3.471	10.438	10.452
Rated generator output frequency f (Hz)	16	48	49.92
Efficiency η (%)	93.09	98.41	98.34
Specific electric loading A (A/mm)	109.99	107.72	106.41
Armature current density J_s (A/mm^2)	4.66	5.02	4.99
Armature thermal load (A^2/mm^3)	512.24	540.98	531.07
Cogging torque (N.m)	958.54	0.23	0.01
Maximum air-gap flux density $\hat{B}_\delta$ (T)	0.46	0.52	0.49
Maximum magnet flux density $\hat{B}_m$ (T)	0.48	0.58	0.64
Maximum statorteeth flux density $\hat{B}_t$ (T)	0.95	1.43	1.36
Maximum statoryoke flux density $\hat{B}_{sy}$ (T)	1.10	1.11	1.07
Maximum rotoryoke flux density $\hat{B}_{ry}$ (T)	1.10	1.11	1.10
Total loss (kw)	742.52	161.55	168.87
Dimension specification			
Air gap diameter D_s (m)	10.622	2.547	1.743
Active length L_s (m)	1.498	0.512	0.391
Slot width b_s (mm)	27.5	11.5	11.2
Slot height h_s (mm)	86.9	62.8	65.8
Stator yoke height h_{sy} (mm)	27.30	148.65	333.05
Rotor yoke height h_{ry} (mm)	48.25	167.65	361.25
Magnet width b_m (mm)	140.72	552.61	1082.83
Magnet height h_m (mm)	21	19.7	38.9
number of slots Q	600	432	288
Number of slots per pole & phase q	1	12	24
Mechanical air-gap height δ (mm)	10	2	2
Polepitch τ_p (mm)	166.85	666.67	1368.70

continues.

to be equipped with integrated water cooling, which helps to increase the limits of the electrical loading constraint. The winding insulation class *N* with an average temperature rise of 130° C for the rated operation and the maximum hot-spot temperature 200° C is considered for the design limits and power loss calculations. No restriction regarding generator frame sizes is imposed to the problem. It is assumed that the generators outputs are connected to infinite bus. In a real case, the outputs are connected to a converter as an external circuit. The converter's dedicated controller controls the phase angle and amplitude of armature output current to attain higher power factors, maximizing the generator output active power. The generators are all designed for an induced voltage less than the rated terminal voltage, which helps to minimize the permanent-magnet material consumption and weight of generator and to reduce the generator core losses. The optimized design based on the proposed analytical model is performed by MATLAB and validated using ANSYS-RMxprt software to ensure that the generators can stably deliver the desired output power and voltage.

The generator structure weight consists of cooling system, beams, cylinder, shaft, and bearings. Different models for the weight is suggested in the literature.[26] In Hartviksen,[29] the generator structure weight is estimated with a sum of cylinder and beams weights. Because the beams weight is proportional to the generator diameter and the cylinder weight has a relation with the multiplication of the diameter and length, the following experimental equation is used to estimate the weight of structure compared with a known structure weight of a similar generator with the same range of power:

$$m_{str} = \frac{1}{2} m_{str}^0 \left(\left(\frac{D_{so}}{D_{so}^0} \right)^2 + \frac{L_s}{{L_s}^0} \right), \tag{4}$$

where m_{str}^0, D_{so}^0, and ${L_s}^0$ are the weight, outer diameter, and length of the reference generator. The data of reference generator, which is a 10-MW DDPMSG, are obtained from Polinder et al.[30]

3.2.2 | Gearbox optimization

In this section, the objective function is minimization of the cost of active material in gearbox by optimizing the stage gear ratios. The gearbox cost function for a typical three-stage configuration is defined by

$$C_{\text{gearbox}}(\boldsymbol{u}) = \arg\ \min \left(cost_{\text{gear}}(\boldsymbol{u}) \right), \tag{5a}$$

TABLE 6 continued

Generator Specifications	DDPMSG	MSPMSG	HSPMSG
Wedge height h_w (mm)	3	2	2
Stator outer diameter D_{so} (m)	10.857	2.973	2.544
Rotor inner diameter D_{ri} (m)	10.464	2.1677	0.9384
Equivalent core length L_e (m)	1.518	0.516	0.395
Slot pitch τ_s (mm)	55.62	18.52	19.01
Winding specification			
Winding layers	2	2	2
Winding type	Full pitch	Full pitch	Full pitch
Parallel branches	1	1	1
Conductors per slot	2	2	2
Winding connection	star	star	star
Number of winding turns N	600	432	288
Insulation thickness h_i, mm/kv	1	1	1
Material properties			
Magnet density ρ_{pm} (kg/m^3)	7400	7400	7400
Relative permeability of magnet μ_{pm}	1.1	1.1	1.1
Magnet residual flux density B_r	1.23	1.23	1.23
Magnet specific cost c_{pm} (Euro/kg)	80	80	80
Core density ρ_{fe} (kg/m^3)	7650	7650	7650
Relative permeability	B-H curve	B-H curve	B-H curve
Core specific cost c_{fe} (Euro/kg)	16	16	16
Copper density ρ_{cu} (kg/m^3)	8900	8900	8900
Copper specific cost c_{cu} (Euro/kg)	27	27	27
Design parameters			
Core stacking factor k_{fe}	0.97	0.97	0.97
Magnetic pole embrace $(\frac{b_m}{\tau_p})$	0.85	0.85	0.85
Weight and cost specification			
Armature copper weight M_{cu} (ton)	12.077	2.109	2.211
Permanent magnet weight M_M (ton)	6.552	0.494	0.487
Armature core weight M_{fe} (ton)	27.777	5.824	7.206
Rotor core weight M_{fe} (ton)	9.984	4.085	3.703
Total active material weight M_{Active} (ton)	56.390	12.513	13.608
Approximated structure weight $M_{structure}$ (ton)	267.85	52.52	39.79
Total weight M_{tot} (ton)	324.24	65.03	53.40
Total active material cost c_{Active} (MEuro)	1.45	0.25	0.27
Total raw material cost c_{total} (MEuro)	5.74	1.09	0.91

Abbreviations: DPMSG, direct-drive permanent-magnet synchronous generator; HSPMSG, high-speed permanent-magnet synchronous generator; MSPMSG, medium-speed permanent-magnet synchronous generator.

$$cost_{gear}(\boldsymbol{u}) = cost_{stage1}(\boldsymbol{u}) + cost_{stage2}(\boldsymbol{u}) + cost_{stage3}(\boldsymbol{u}), \tag{5b}$$

where u is vector of the optimization variables. $cost_{gear}$ is total raw material cost of the gears of gearbox stages in Euro. The variables in Equation (5) are described as

$$\boldsymbol{u} = [u_1, u_2, u_3]^T, \tag{6a}$$

$$cost_{stage}^{planetary} = c_{gear} m_{gear}^{planetary}, \tag{6b}$$

$$cost_{stage}^{parallel} = c_{gear} m_{gear}^{parallel}, \tag{6c}$$

where c_{gear} is the unit cost of the gears material and $m_{gear}^{planetary}$ and $m_{gear}^{parallel}$ represent the weights of planetary and parallel stages, respectively, which is defined as the function of optimization variables using the model described in Nejad et al[31] as

$$m_{gear}^{planetary}(u) = \frac{2\rho_{fe} Q_S}{k}\left(\frac{1}{B} + \frac{1}{B\left(\frac{u}{2}-1\right)} + \left(\frac{u}{2}-1\right) + \left(\frac{u}{2}-1\right)^2 + k_r\frac{(u-1)^2}{B} + k_r\frac{(u-1)^2}{B\left(\frac{u}{2}-1\right)}\right), \tag{7a}$$

$$m_{gear}^{parallel}(u) = \frac{2\rho_{fe} Q_P}{k}\left(1 + \frac{1}{u} + u + u^2\right), \tag{7b}$$

where Q_S and Q_P are the input torques to the sun and pinion for planetary and parallel stages, respectively. u is the gear ratio, B is number of planets of the planetary stage, and k_r is a ring scaling factor of the planetary stage. k is the intensity of tooth loads factor. The overall active material weight for a sample three-stage gearbox with two planetary and one parallel stages is calculated as

$$\begin{aligned} m_{gears}(u) = {} & \frac{2\rho_{fe}Q_0}{k}\frac{1}{u_1}\left(\frac{1}{B}+\frac{1}{B\left(\frac{u_1}{2}-1\right)}+\left(\frac{u_1}{2}-1\right)+\left(\frac{u_1}{2}-1\right)^2+k_r\frac{(u_1-1)^2}{B}+k_r\frac{(u_1-1)^2}{B\left(\frac{u_1}{2}-1\right)}\right) \\ & +\frac{2\rho_{fe}Q_0}{k}\frac{1}{u_1u_2}\left(\frac{1}{B}+\frac{1}{B\left(\frac{u_2}{2}-1\right)}+\left(\frac{u_2}{2}-1\right)+\left(\frac{u_2}{2}-1\right)^2+k_r\frac{(u_2-1)^2}{B}+k_r\frac{(u_2-1)^2}{B\left(\frac{u_2}{2}-1\right)}\right) \\ & +\frac{2\rho_{fe}Q_0}{k}\frac{1}{u_1u_2u_3}\left(1+\frac{1}{u_3}+u_3+u_3^2\right). \end{aligned} \tag{8}$$

Equation (8) is obtained by the sum of the weights of two planetary stages and one parallel stage as described in Equation (7). The input torque applied on the sun/pinion of each gearbox stage is replaced in the weight function of the stage by applying the gear ratio of the previous stages on the main shaft torque Q_0. To derive Equation (8), it is important to notice the sun/pinion is the output gear of the planetary/parallel gear stage.

The above described optimization problem is solved subject to constraints related to the gear ratio of each stage and the overall gear ratio. The outputs of the problem are the optimized gear ratios, weight, and cost. The resultant is a constrained nonlinear multivariable nonconvex optimization problem. Because the aforedescribed disciplined nonconvex problem shows a convex behavior in multidimensional graphical illustration of the objective function and constraints in the defined range of optimization variables, it is possible to find the global optimizer. MATLAB *fmincon* numerical optimization solver is used to find the global optimizer.

The replacement of the third parallel stage in MSPMSG drivetrain with a planetary stage in HSPMSG helps to reach higher gear ratios and reduce weight and size with compact design features of planetary gears. The disadvantages of planetary gearboxes are their complexity and sensitivity to manufacturing errors and elastic deformations in the shafts, bearings, and gearbox cage so that a planetary gearbox performs the best only if equal load sharing between planets is achieved.[32] The optimized three-planetary stages gearbox for HSPMSG drivetrain and two-planetary and one-parallel stage gearbox for MSPMSG drivetrain based on the explained model and the proposed optimization approach are evaluated as the case studies in Section 4. The gearboxes optimized designs are validated using the KISSsoft gear design software, and the overall geometry, weight, cost, and efficiency are compared for the different topologies.

3.2.3 | The first torsional natural frequency of drivetrain

To ensure that the different designed drivetrain technologies execute a safe operation without any danger of resonance due to external/internal excitations, the first torsional natural frequency of three under consideration drivetrain systems is studied. The first torsional frequency is calculated by using a simplified two-mass model. The gearbox is modelled with the gear ratio and the stiffness of the connecting links to the rotor and generator are modelled, but the moment of inertia and stiffness of the gearbox are neglected. The moment of inertia of the gearbox is negligible compared with the moment of inertia of the generator so that it does not have any considerable impact on the first drivetrain torsional mode. The first torsional frequency by using a two-mass model is calculated by[33]

$$f_1^{tor} = \frac{1}{2\pi}\sqrt{k_{eq}\frac{J_r+\alpha^2J_{gen}}{\alpha^2J_rJ_{gen}}}, \quad k_{eq} = \frac{\alpha^2k_rk_{gen}}{k_r+\alpha^2k_{gen}}, \tag{9}$$

where k_{eq} is the equivalent shaft stiffness in the rotor side, J_r and J_{gen} are the moment of inertia of rotor and generator, k_r and k_{gen} are the shaft stiffness of rotor and generator, and α is inverse of the gear ratio.

The first torsional natural frequency of drivetrain of the three under consideration topologies obtained by the above model is validated by using a three-mass model in Simpack software, which models the moment inertia of the gearbox to see how it can influence the first mode.

4 | NUMERICAL SIMULATIONS

4.1 | Optimized generator specification

The results of the three optimized generator designs based on DDPMSG, MSPMSG, and HSPMSG using the proposed analytical approach are listed in Table 6. The three optimized designed generators are validated by ANSYS-RMxprt. The terminal voltage and power-angle characteristics of the designed generators, which show that the three generators can stably deliver the designed power with the target voltage, are shown in Figure 4. The power angle characteristic shows the relation between the power output of the generator P_e and the power angle δ. The power angle is the angle between the generator induced voltage at the air gap and the terminal voltage. When the input mechanical power increases, the power angle increases to counterbalance the input power by the increase of the generated electrical power, where there is a $\delta = \pi/2$ *rad*

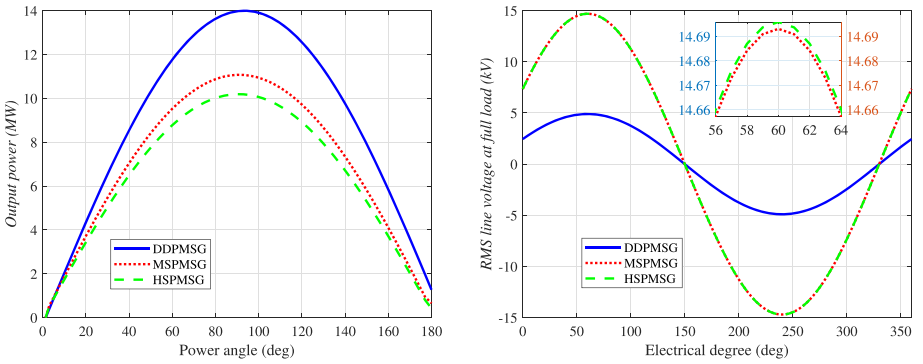

(A) P_e vs. δ (B) V_L vs. Degree

FIGURE 4 Characteristic curves of the designed generators. DDPMSG, direct-drive permanent-magnet synchronous generator; HSPMSG, high-speed permanent-magnet synchronous generator; MSPMSG, medium-speed permanent-magnet synchronous generator [Colour figure can be viewed at wileyonlinelibrary.com]

limit that any exceedance causes a loss of synchronism and instability. The curve demonstrated in Figure 4A is the power-angle characteristic obtained from the validated model in ANSYS-RMxprt software and shows that the three designed generators are all able to deliver the designed 10 MW power but at different power angles. The designed points on the power-angle characteristic of the generators are the optimal operation by the consideration of efficiency and power factor in the optimization problem under a rated operation. The operating point in the three designs also has a safe distance from the power angle limit $\delta = \pi/2$ *rad*. Although the designed generators can give higher power especially in DDPMSG, it will not result in a desirable operation regarding a much lower efficiency. The frequency converter can also influence on the power factor and subsequently the power angle. The generator terminal voltage is also an important constraint in the optimized design problem so that the designed generators must be able to deliver the rated power at the rated voltage level, which the generator is designed for. Figure 4B shows one cycle of the terminal line voltage ($V_{Line} = \sqrt{3}V_{Phase}$) of the three designed generators validated by ANSYS-RMxprt.

As it can be seen in Table 6, a transition from the low-speed to high-speed generator helps to save weight by reduction of diameter and length of the generator although the required stator and rotor yokes height increases. For higher speed generators, the reduction of the number of poles still decreases the diameter and length of machine; however, the rise in the stator and rotor yokes height exceeds the amount of weight saved by the reduced diameter and length. Consequently, the weight of active material in HSPMSG is increased, but the total weight including the weight of structure is still less than MSPMSG technology. Considerable reduction of weight and raw material cost in the generators designed for higher operational speeds and improved efficiency and torque oscillations are observed based on the simulation results.

The efficiency of generator in the optimized analytical design approach is considered as a constraint so that the design solution has to fulfill the minimum requirements regarding the power loss and efficiency. For this purpose, in the design code, the components of generator power loss consisting of winding loss, rotor and stator cores losses (hysteresis and eddy current losses), magnet losses, additional losses (stray losses), and friction and windage losses are modelled at rated load operation. The optimized design is then validated by the ANSYS-RMxprt analytical design software to ensure that the designed generator can supply the designed power at the specified voltage. This software makes it possible to check a wide range of parameters related to the generator operation including but not limited to flux densities in different places, electric loading, thermal loading, induced and terminal voltage, power factor, total harmonic distortion, power losses, and efficiency. The values of efficiency given in the paper are the verified results obtained by ANSYS. It is worth noting that maintaining the same efficiency for the low-speed generator needs more increase in volume compared with higher speed generators. The latter makes high-efficiency DDPMSG technology for high-power applications infeasible or inefficient. The voltage and frequency for the design of DDPMSG are selected less than the two other generators, to help the minimum weight and cost design. The design voltages are selected so that the output voltage of converter place in a standard voltage level based on the standards.[34,35] Regarding the reduced rotational speed in DDPMSG and the direct relationship between the induced voltage and speed, it is not efficient to design the direct-drive generator with the same voltage level used for medium-speed and high-speed generators design. The relative root mean square (RMS) value of the fundamental component of the induced voltage is given by[27]

$$E_r = \sqrt{2}k_w\omega_s N_{ph}\frac{D_s}{2}L_e B_\delta^1, \tag{10}$$

where k_w is the winding factor, ω_s is the rotational speed in *rad*/*s*, and B_δ^1 is the RMS value of the fundamental component of the air gap flux density. Therefore, the increase of induced voltage means the rise in the number of turns (more winding weight), the length of the machine (more core weight), and the air gap flux density (more magnet weight). The latter increases the weight and cost of design. A power transformer in the wind turbine is used to adjust the converter output voltage to the voltage at point of common coupling (PCC) so that the reduced voltage of DDPMSG and consequently the reduced converter output voltage does not cause any problem if the voltage is selected among the standard voltages.

The design for a reduced output frequency also helps to reduce the number of poles and consequently the diameter and weight of generator. The latter is possible, because the power converter can adjust the output frequency if the frequency is in the converter operating range. Therefore, the design of DDPMSG for a lower voltage level and frequency is practical and results in the minimum weight design of the direct-drive generator. The other two machines, that is, MSPMSG and HSPMSG are designed for the same standard voltage level. Similar loading conditions

TABLE 7 Gearbox optimization results

Gearbox Specifications	MSPMSG		HSPMSG
Technical specification			
Type	Two planetaries and one parallel	Three planetaries	Three planetaries
Overall gear ratio	1:50	1:50	1:156
Rated power (MW)	10	10	10
Rated input shaft speed n (rpm)	9.6	9.6	9.6
Rated input shaft torque Q (MN.m)	9.947	9.947	9.947
Efficiency η (%)	97.3	97.3	98.1
Gear specification of the first stage			
Gear type	Planetary	Planetary	Planetary
Gear ratio	1:3.524	1:3.231	1:4.333
Number of planets	5	5	5
Normal module	32	45	28
Normal pressure angle (degree)	23.3	27.1	24.6
Helix angle (degree)	0	0	0
Center distance a (m)	0.917	1.140	1.027
Sun gear facewidth b_1 (m)	0.533	0.316	0.568
Planets facewidth b_2 (m)	0.514	0.297	0.552
Ring gear facewidth b_3 (m)	0.533	0.316	0.568
Number of teeth, sun	33	31	34
Number of teeth, planet	23	17	37
Number of teeth, ring	82	69	111
Profile shift coefficient, sun	0.217	0.664	0.446
Profile shift coefficient, planet	0.493	0.907	0.866
Profile shift coefficient, ring	0.249	0.312	0.555
Weight m_{gear}^{51} (ton)	17.53	15.01	28.11
Efficiency η (%)	99	98.9	99.4
Gear specification of the second stage			
Gear type	Planetary	Planetary	Planetary
Gear ratio	1:4.804	1:3.4560	1:6
Number of planets	3	3	3
Normal module	25	28	25
Normal pressure angle (degree)	24.3	23.7	23.4
Helix angle (degree)	0	0	0
Center distance a (m)	0.696	0.819	0.704

continues.

are considered for design of the three generators to reach a fair comparison between them. Mechanical losses including friction and windage are neglected.

4.2 | Optimized gearbox specification

The optimized medium-speed and high-speed gearboxes specifications including the geometrical and technical data of the stages, respectively for 10-MW MSPMSG and HSPMSG wind turbine drivetrain systems using the analytical model described in Section 3 are specified in Table 7. The results validated using KISSsoft software show that even though the multistage gearbox for the HSPMSG drivetrain is designed for a higher gear ratio, it can still slightly reduce the total weight and improve the efficiency of the gearbox. The change in the weight scaling factor applied to model the structure weight of the two different gearboxes can slightly affect the results about the gearbox weight. As it can be seen, a transition from medium-speed to high-speed gearbox can help to slightly improve the efficiency and weight. To provide a fair comparison, because there was no reference found, which prohibits the utilization of three planetary stages instead of two planetary and one parallel stages to realize a medium-speed gearbox, the optimized results of another medium-speed topology based on three planetary stages is added to Table 7.

The values of gearbox efficiency are the validated values calculated by KISSsoft after the implementation of the optimized model in the software environment. KISSsoft is an analytical tool that calculates the power loss and heat dissipation of each gear stage according to the ISO/TR 14179 standard. The software analytical efficiency calculations are elaborated by Langhart et al.[36]

4.3 | Comparison between different PMSG-based drivetrain technologies

The overall drivetrain weight, cost, and efficiency for DDPMSG, MSPMSG, and HSPMSG are summarized in Table 8 and graphically compared in Figures 5A to 5C. As it can be seen, moving from the direct-drive technology towards the medium-speed, the drive train weight, raw material cost,

TABLE 7 continued.

Gearbox Specifications		MSPMSG	HSPMSG
Sun gear facewidth b_1 (m)	0.466	0.331	0.415
Planets facewidth b_2 (m)	0.450	0.316	0.401
Ring gear facewidth b_3 (m)	0.466	0.331	0.415
Number of teeth, sun	23	34	19
Number of teeth, planet	31	23	36
Number of teeth, ring	88	83	95
Profile shift coefficient, sun	0.176	0.283	0.430
Profile shift coefficient, planet	0.754	0.535	0.285
Profile shift coefficient, ring	-0.157	-0.137	0.772
Weight m_{gear}^{S2} (ton)	9.06	6.74	9.26
Efficiency η (%)	99.2	99.2	99.3
Gear specification of the third stage			
Gear type	Parallel	Planetary	Planetary
Gear ratio	1:2.95	1:4.4775	1:6
Number of planets	…	3	3
Normal module	40	18	14
Normal pressure angle (degree)	20	22.7	23.3
Helix angle (degree)	0	0	0
Center distance a (m)	1.177	0.495	0.394
Sun/pinion facewidth b_1 (m)	0.622	0.223	0.201
Planets/gear facewidth b_2 (m)	0.599	0.212	0.195
Ring facewidth b_3 (m)	…	0.223	0.201
Number of teeth, sun /pinion	15	25	19
Number of teeth, planet/gear	44	29	36
Number of teeth, ring	…	86	95
Profile shift coefficient, sun/pinion	0.377	0.092	0.225
Profile shift coefficient, planet /gear	-0.451	0.441	0.471
Profile shift coefficient, ring	…	0.405	0.595
Weight m_{gear}^{S3} (ton)	12.28	2.04	1.43
Efficiency η (%)	99.1	99.2	99.4
Design parameters			
Intensity of tooth loads factor	4×10^6	4×10^6	4×10^6
Ring scaling factor	0.4	0.4	0.4
Housing, bearings & lubrication scale factor	0.2	0.2	0.2
Material properties			
Material	Case carburized steel	Case carburized steel	Case carburized steel
Density (kg/m^3)	7850	7850	7850
Specific cost c_{gear} (Euro/kg)	16	16	16
Weight and cost specification			
Total gears weight (ton)	38.87	23.79	38.80
Moment of inertia $(Mkg.m^2)$	1.24	0.25	0.36
Total weight (ton)	46.64	28.55	46.56
Total raw material cost (MEuro)	0.75	0.46	0.74

Abbreviations: DPMSG, direct-drive permanent-magnet synchronous generator; HSPMSG, high-speed permanent-magnet synchronous generator.

efficiency and electromagnetic torque oscillations are significantly improved. A transition from the medium-speed to the high-speed generator still helps to improve all the aforementioned properties.

To reduce fatigue damage and noise and comply with standard limits, a suppression to the permissible level 2% for electromagnetic torque oscillations is required.[37] Torque oscillation in surface-mounted PMSGs mainly comes from two sources[38,39]:

1. Cogging effect due to the variable permeance of the air gap and
2. Distortion of sinusoidal distribution of air gap flux density due to saturation, current ripple resulting from pulse width modulation (PWM), and low power quality of the grid.

Cogging torque resulting from cogging effect is an important component of torque oscillations in PMSGs, which can be improved by the proper design. As it can be seen in Table 8, the designed generators fulfill the torque oscillation requirements. However, the ratio of the cogging to the average torque reduces by the increase of gear ratio. The fundamental cogging frequency for the PMSG with integer-slot windings and

TABLE 8 Drivetrain optimization results

Drivetrain Technology	DDPMSG	MSPMSG		HSPMSG
Gearbox configuration	No gearbox	Planetary-planetary-parallel	Three planetaries	Three planetaries
Generator weight (ton)	324.24	65.03	65.03	53.40
Generator cost (MEuro)	5.74	1.09	1.09	0.91
Gearbox weight (ton)	0	46.64	28.55	46.56
Gearbox cost (MEuro)	0	0.75	0.46	0.74
Total weight (ton)	324.24	111.67	93.58	99.96
Total cost (MEuro)	5.74	1.84	1.55	1.66
Electromagnetic torque oscillation (%)	0.00897	0.00011	0.00011	0.00001
Rated efficiency (%)	93.09	95.75	95.75	96.47

Abbreviations: DPMSG, direct-drive permanent-magnet synchronous generator; HSPMSG, high-speed permanent-magnet synchronous generator; MSPMSG, medium-speed permanent-magnet synchronous generator.

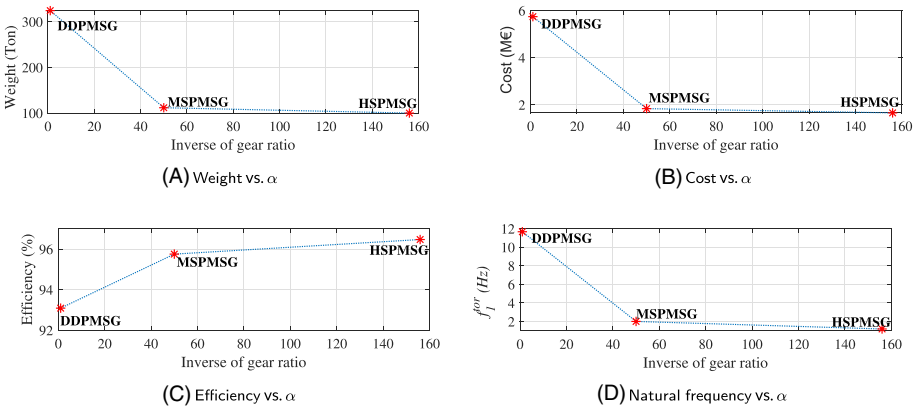

FIGURE 5 Comparison between different drivetrain technologies: DDPMSG, MSPMSG and HSPMSG. DPMSG, direct-drive permanent-magnet synchronous generator; HSPMSG, high-speed permanent-magnet synchronous generator; MSPMSG, medium-speed permanent-magnet synchronous generator [Colour figure can be viewed at wileyonlinelibrary.com]

surface-mounted magnets is calculated by[40]

$$f_{cog} = Q\frac{2f_{in}}{p}, \tag{11}$$

where Q is number of slots, f_{in} is generator input frequency, and p is number of poles. It can be seen that the cogging torque frequency depends on the input speed, but in rated operation, the cogging torque frequencies for DDPMSG, MSPMSG, and HSPMSG are 0.96, 57, and 3600 Hz, respectively. The higher cogging torque frequency of higher speed generators reduces the probability of coincidence on the natural frequencies of the drivetrain main bearings and the generator bearings' inner ring, outer ring, and rolling elements (see the associated failure modes in Table 4). Regarding the higher shaft first torsional natural frequency in DDPMSG, it is doubted that the cogging frequency can coincide this frequency. The type of main bearings in the wind turbines are mostly spherical roller bearings. These bearings have different defect frequencies due to out-of-round rotating, roller irregularity, and outer and inner race irregularities. For the under consideration 10-MW turbine, the defect frequency of these modes can start from a fraction of hertz and rise up to few hertz. The cogging torque in DDPMSG can cause fatigue damage to bearing components due to the possibility of coincidence with main bearing defect frequencies. For higher speed generators in MSPMSG and HSPMSG technologies, it is also possible that cogging torque coincides the gears mesh frequencies, which can affect the gear teeth fatigue life. However, in the designed medium-speed and high-speed gearboxes, the mesh frequencies of generator side gear stage are 120 and 474 Hz, respectively, which keep a safe distance from the rated fundamental cogging torque frequencies. The presence of gearbox results in a longer transmission path between the external excitation source initiated from the rotor (aerodynamic torque and forces) and the generator side (electromagnetic torque and forces), which are transmitted to the generator and rotor side components, respectively, which can reduce the amplitude of drivetrain external excitations. The latter can affect the probability of failure of generator and rotor side components (eg, main bearings) due to those external excitations. The increased defect frequencies of the generator bearings due to the rise in the rotational speed naturally immunizes these components against the loads applied on the drivetrain by rotor as a result of synergistic impacts of wind, waves, and structural motions, which all appear with a low frequency content. The latter shows some potentials to improve the reliability of main bearings and generator in the drivetrain, although the appearance of gearbox as a new serial component has a negative impact on the reliability of drivetrain. Therefore, it is challenging to compare the overall reliability of the under consideration drivetrain systems. In the continued part, the possibility of resonance by using the three designed drivetrain systems is investigated.

There is a coupling between gearbox and generator in the geared wind turbine drivetrain systems used for reducing torsional vibration and accommodating misalignment. The coupling between generator and gearbox could suppress the high-frequency excitations initiated by the generator due to distortion of air gap flux in order not to be transmitted to the rest of the drivetrain. Those frequencies happen mostly in harmonics of generator output frequency. The cogging frequency in MSPMSG and HSPMSG has a high-frequency nature and is isolated by the coupling from the rest of the drivetrain although there is not any possibility for this frequency to coincide with the first torsional frequency

TABLE 9 The first torsional natural frequency of drivetrain, and the excitation sources

Drivetrain Technology	DDPMSG	MSPMSG	HSPMSG
Generator moment of inertia J_{gen} (kg.m^2)	456965.65	6286.71	1888.30
First torsional natural frequency -by two mass model (Hz)	11.66	2.01	1.20
First torsional natural frequency -by three mass model in Simpack (Hz)	11.66	1.93	1.19
1P rotational frequency (Hz)	0-0.16	0-0.16	0-0.16
3P rotational frequency (Hz)	0-0.48	0-0.48	0-0.48
Wind (Hz)	0-0.02	0-0.02	0-0.02
Wave (Hz)	0.05-0.2	0.05-0.2	0.05-0.2
Electromagnetic torque oscillations (Hz)	0-10000	0-10000	0-10000
Gear mesh frequency-first harmonic at rated speed (Hz)	…	18-120	23-474
Bearing defect frequency-first harmonic at rated speed (Hz)	0.16-8	0.16-170	0.16-500

Abbreviations: DPMSG, direct-drive permanent-magnet synchronous generator; HSPMSG, high-speed permanent-magnet synchronous generator; MSPMSG, medium-speed permanent-magnet synchronous generator.

due to the high-frequency nature of cogging torque in geared drivetrain technologies. In DDPMSG, there is normally no mechanical torsional vibration isolator in the drivetrain system. As a result, the generator torsional vibrations including low frequency (due to cogging torque) and higher frequencies (due to saturation, power converter switching, and power grid) transmit to the rotor side of the drivetrain. The latter can influence on the drivetrain lifetime specially in higher powers with smaller values of the first drivetrain torsional frequency, generator cogging torque frequency, and generator output frequency.

Active vibration dampers are another drivetrain torsional vibration damping mechanism, which are used to mitigate the impact of the significant torsional vibrations on the drivetrain due to aerodynamic torque oscillations (usually, the frequencies that are considered to be damped by active dampers are the first drivetrain torsional mode and first blade in plane mode) by compensation of them in the generator electromagnetic torque set point. These dampers are generally band-pass filters, which are tuned around some prespecified frequencies. If these mechanical oscillations do not get compensated in the generator torque, the consequent electric power oscillations not only reduces the power quality but also can interact with power system modes and cause resonances with the electric circuits frequencies, which can cause high voltages and currents and damage the electric components. Instead of these compensations on torque through active dampers, some turbines use passive parallel band-stop filters in the frequency converter system to filter the frequencies of the aerodynamic torque oscillations from the output electric power. To our best knowledge, the active dampers do not influence on the torsional vibrations initiated by generator. In direct-drive technologies, due to the lack of coupling, there is no mechanism to suppress the transmission of generator vibrations to the rotor side. In 10-MW DDPMSG, the cogging frequency can coincide with the defect frequencies of the main bearings and there is no mechanism reported in the literature of direct-drive drivetrain systems to isolate this low frequency range excitations that are initiated from the generator side.

4.4 | The first torsional natural frequency of drivetrain and resonance analysis

ANSYS-Maxwell moment of inertia calculation package is used to obtain a good estimation of the generator moment of inertia for the designed generators. The first torsional frequency of designed DDPMSG, MSPMSG, and HSPMSG drivetrains is presented in Table 9 and graphically illustrated in Figure 5D. The rotor and tower flexibilities are neglected in the calculation of the first torsional frequencies.

The excitations that influence on the drivetrain operation come from different sources, for example, turbine rotational motion, motions induced by structural resonances, wind- and wave-induced motions, the electromagnetic torque oscillation resulted by cogging torque/saturation/converter system/power grid, and the drivetrain internal excitations due to the gears mesh frequencies and the bearings defect frequencies. For the drivetrain system, the most unfavorable operating condition happens when the rotor rotational frequency (1P) coincides the drivetrain first torsional frequency. The other source of excitation that can affect the rotor torque comes from the tower shadow effect, which occurs with blade passing frequency 3P. The tower bending (TB) frequency excited by the 1P or 3P rotational frequencies is another source of excitation in a spar floating platform.[41] An excited TB natural frequency causes motions that induce a moment component on the rotor torque. Wave is another excitation source in offshore wind turbines so that waves at sea have significant energy at periods of 5 to 20 seconds. An example of wave impacts is nacelle side-side motion developed by sway and rolling motions, which has a low frequency inherent. The natural periods of wind excitations also change from a fraction of a minute for turbulent fluctuations to some hours due to diurnal effects. The impacts of the generator cogging torque on the drivetrain components was discussed earlier. The power grid and converter system are the other excitation sources that influence on the generator electromagnetic torque and consequently the moment on the shaft. The latter can have different reasons, for example, grid voltage drops, swells and harmonics, and the harmonics in the current resulted by the PWM frequency converter,[42] which happen with higher frequencies potentially starting from the first or the higher order harmonics of $\frac{np}{120}$ up to a few thousands of hertz depending on the grid power quality, converter topology, the modulation technique, and switching frequency.[43] n is the generator rotational speed. The internal excitations due to any excited bearing frequencies (main bearings, gearbox, and generator bearings) or gear mesh frequencies of the gearbox stages can work as an impact that could excite the system natural frequencies and the defect frequencies of the other components. The excitation sources with the same frequencies can cause more complicated impacts. Combined impacts of different excitations with the same

TABLE 10 Environmental conditions for drivetrain analysis

EC	1	2	3	4
U_w (m/s)	7	9	11	15
H_s (m)	2.5	3.5	3.5	3.5
T_p (s)	6.5	7.5	7.5	11.5

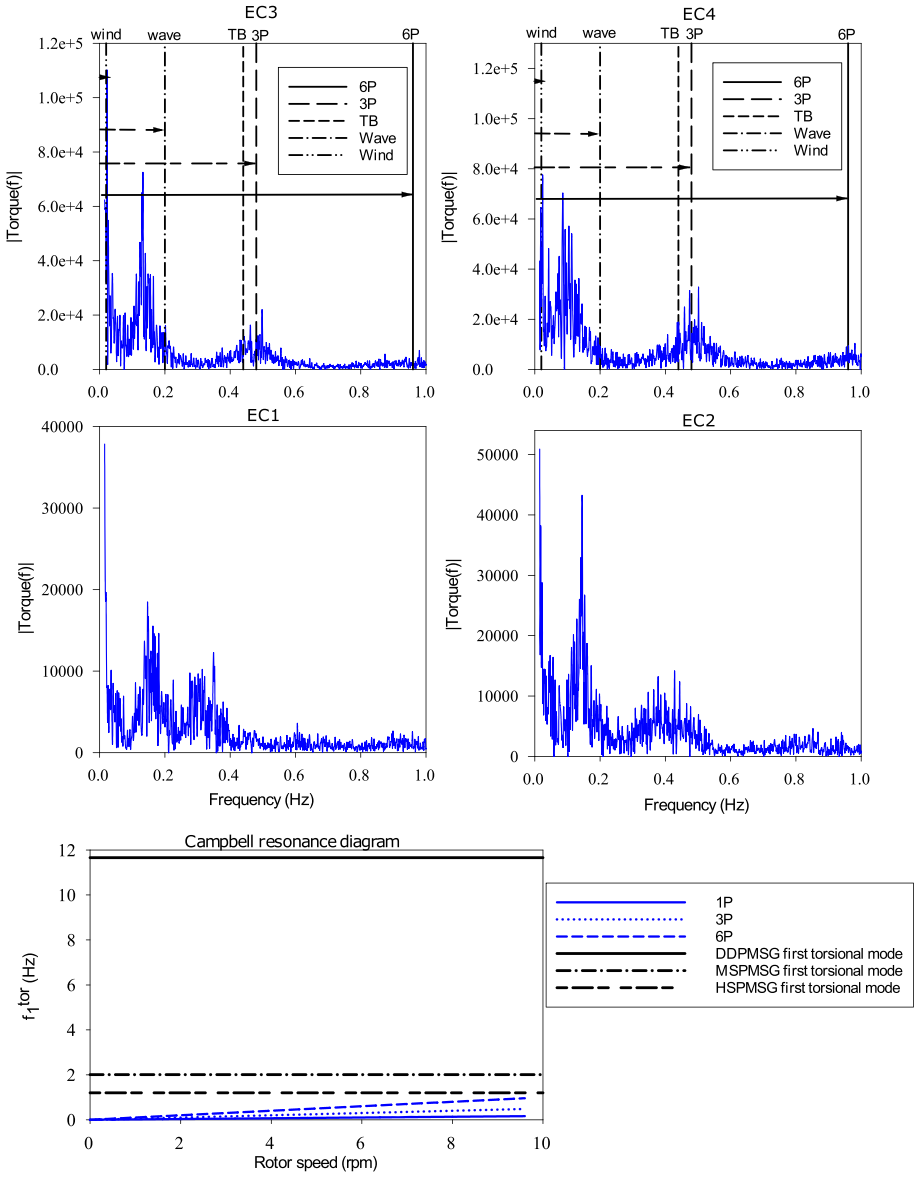

FIGURE 6 Rotor torque frequency spectrum analysis of 10-MW spar floating offshore wind turbine in different environmental conditions and associated resonance diagram. DPMSG, direct-drive permanent-magnet synchronous generator; HSPMSG, high-speed permanent-magnet synchronous generator; MSPMSG, medium-speed permanent-magnet synchronous generator [Colour figure can be viewed at wileyonlinelibrary.com]

frequencies can result in a coupled effect by producing other frequencies described as beating effect in Thomson.[44] An overview of the excitation sources for 10-MW spar floating wind turbine is presented in Table 9.

In order to determine which loads can excite the first torsional natural frequency of drivetrain, an effective approach could be to study the drivetrain response by using a frequency-domain analysis. For this purpose, the rotor torque data of the DTU 10MW reference wind turbine with a spar floating platform obtained from SIMA global simulation software is used, and the impacts on the drivetrain are studied using a decoupled analysis. Decoupled analysis approach is explained in detail in Nejad et al.[45] This model is very useful to study the consequences of the drivetrain torsional excitations induced by aerodynamic loads and structural motions. The specification of the spar floating platform used in the global simulations is given by Hegseth et al.[41] To study the impact of wind and wave, four different environmental conditions are simulated as listed in Table 10. For different wind speeds U_w within the operational range of the turbine, the most probable values of significant wave height H_s and peak period T_p are selected for the global simulations. In order to analyze how the different loads influence on the response, the frequency spectrum of rotor torque for the different operating conditions is shown in Figure 6. The frequency spectrum of the signal in frequencies lower than 1 Hz is selected and shown because the most significant energy of the rotor torque was observed in this range. The possible resonances due to external excitations for the three optimally designed drivetrain systems are demonstrated by the Campbell diagram in Figure 6.

The torque components induced by tower shadow, TB, wind, and wave are depicted in the figure. As it can be seen, the wave- and wind-induced components are very low frequency so that they cannot excite the torsional modes of any of the three under consideration drivetrain systems. The other excitations with considerable energy (including 1P, TB, 3P, and 6P) happen at the frequencies less than 1 Hz so that none of the designed DDPMSG, MSPMSG, and HSPMSG drivetrain technologies are affected by aerodynamic loads and structural excitations. A larger distance between the drivetrain natural frequency and the aerodynamic loads is an advantage of lower speed generator technologies, where DDPMSG outperforms the other drivetrain systems. On the other side, for the drivetrain with higher first torsional frequency, it would be more susceptible to excitations with generator torsional vibration frequencies, especially in the direct drive technology in which there is no coupling between the generator and rotor to suppress the generator electromagnetic torque vibrations. In lower speed generator technologies, in order to reduce the generator size, the number of poles is reduced. Consequently, the generator output frequency is reduced. For instance, the generator output frequency of the DDPMSG design in the paper is 16 Hz. The generator reduced output frequency and simultaneously increased first torsional frequency (eg, 11.66 Hz for the designed DDPMSG), which is a drawback of drivetrain technologies based on lower speed generators. During operations at speeds lower than the rated value, it is quite possible that the frequency of the generator-induced voltage coincides with the first natural frequency, which is not a recommended operation. Operations at this speed or any transition over it can cause large vibrations in the system. The nontorsional excitation sources , for example, bearings and gears, have also a potential to induce torque vibrations at bearing defect frequencies and gear mesh frequencies, respectively. The higher the value of the first torsional frequency, the more the possibility of coincidence with those frequencies. For example, in DDPMSG, it is possible that the second harmonic of main bearings roller irregularity frequency coincides with the first torsional frequency. From this perspective, higher speed generators could exhibit a higher performance. Therefore, with respect to dynamic response and resonance possibility, MSPMSG seems to be a better compromise.

5 | DISCUSSIONS AND CONCLUDING REMARKS

The optimized analytical 10-MW drivetrain designs for three different PMSG-based drivetrain topologies, that is, DDPMSG, MSPMSG, and HSPMSG, were explained and compared, and the feasibility of application in spar floating offshore wind turbines was studied. The results showed that utilization of gearbox can improve both the economics and operations of the wind turbine in 10-MW floating offshore wind turbines based on the following proven reasons:

1. It helps to reduce the weight of the drivetrain system,
2. It reduces the raw material cost of the drivetrain,
3. It can result in a better dynamic performance and reduce the possibility of resonance in the drivetrain due to the coincidence of the excitation frequencies (initiated by aerodynamic torque and electromagnetic torque) with the first drivetrain torsional frequency and the individual components defect frequencies,
4. Higher speed generator technologies in MSPMSG and HSPMSG drivetrain systems help to improve the overall drivetrain efficiency.

By considering the interactions between the drivetrain components, it was discussed how a medium-speed gearbox can improve some drivetrain failure modes concerning with the generator and the main bearings. However, new failure modes due to the presence of gearbox will also appear in the geared drivetrain systems. Regarding the lack of any operational data at this power range, the weakness of simulation tools in modelling of such complex dynamical system, and insufficient knowledge on loads in floating applications, it is challenging to compare the reliability of different drivetrain technologies. Future work will be devoted on investigating the optimal gear ratio for the PMSG drivetrain for 10-MWturbine and comparing the expected lifetime of different PMSG drivetrain systems by a thorough reliability analysis for floating offshore applications.

ACKNOWLEDGMENT

The authors would like to thank John Marius Hegseth of Norwegian University of Science and Technology, Trondheim, Norway, for providing the 10-MW spar floating wind turbine global analysis simulation results.

ORCID

Farid K. Moghadam https://orcid.org/0000-0002-0795-6887
Amir R. Nejad https://orcid.org/0000-0003-0391-8696

REFERENCES

1. IRENA I. *Renewable Power Generation Costs in 2017*. Abu Dhabi: International Renewable Energy Agency; 2018.
2. Note on technology costs for offshore wind farms and the background for updating CAPEX and OPEX in the technology catalogue datasheets. Danish Energy Agency; 2018.
3. Guo Y, Parsons T, King R, Dykes K, Veers P. *Analytical Formulation for Sizing and Estimating the Dimensions andWeight of Wind Turbine Hub and Drivetrain Components*. Golden, CO (United States): National Renewable Energy Lab.(NREL); 2015.

4. Guo Y, Parsons T, Dykes K, King R. A systems engineering analysis of threeâĂŘpoint and fourâĂŘpoint wind turbine drivetrain configurations. *Wind Energy*. 2017;20(3):537-50.
5. McKenna R, Ostman P, Leye VD, Fichtner W. Key challenges and prospects for large wind turbines. *Renew Sustain Energy Rev*. 2016;53:1212-1221.
6. Cheng M, Zhu Y. The state of the art of wind energy conversion systems and technologies: a review. *Energy Convers Manag*. 2014;88:332-347.
7. Gorginpour H, Oraee H, McMahon R. Electromagnetic-thermal design optimization of the brushless doubly fed induction generator. *IEEE Trans Ind Electron*. 2014;61:1710-1721.
8. Abrahamsen A, Liu D, Magnusson N, et al. Comparison of levelized cost of energy of superconducting direct drive generators for a 10-MW offshore wind turbine. *IEEE Trans Appl Supercond*. 2018;28:1-5.
9. Bak C, Zahle F, Bitsche R, et al. Description of the DTU 10 MW reference wind turbine. *DTU Wind Energy Report-I-0092*; 2013.
10. Sethuraman L, Maness M, Dykes K. Optimized generator designs for the DTU 10-MW offshore wind turbine using GeneratorSE. In: 35th Wind Energy Symposium; 2017:0922.
11. Rkke A. Permanent Magnet Generators for Marine Current Tidal Turbines. *Ph.D ,thesis*. Norway; 2017.
12. Torsvik J, Nejad A, Pedersen E. Main bearings in large offshore wind turbines: development trends, design and analysis requirements. *J Phys Conf Ser*. 2018;1037:042020.
13. Mayer J, Gerling D. Simulation of arbitrary fault-conditions in PM-machines by generalized unsymmetrical modeling. In: IEEE XXth International Conference on Electrical Machines; 2012:2866-2872.
14. Morgan AW, Wyllie D. A survey of rolling-bearing failures. In: Proceedings of the Institution of Mechanical Engineers, Conference Proceedings, Vol. 184; 1969:48-56.
15. Valavi M, Nysveen A, Nilssen R, Lorenz R, Rlvg T. Influence of pole and slot combinations on magnetic forces and vibration in low-speed PM wind generators. *IEEE Trans Mag*. 2014;5:1-1.
16. Nejad A, Gao Z, Moan T. Fatigue reliability-based inspection and maintenance planning of gearbox components in wind turbine drivetrains. *Energy Procedia*. 2014;53:248-57.
17. Tallian T. On competing failure modes in rolling contact. *ASLE Trans*. 1967;4:418-39.
18. Nejad A, Gao Z, Moan T. On long-term fatigue damage and reliability analysis of gears under wind loads in offshore wind turbine drivetrains. *Int J Fatigue*. 2014;61:116-28.
19. Gao Z, Bingham H, Ingram H, et al. Committee V. 4: Offshore Renewable Energy. In: In Proceedings of the 20th International Ship and Offshore Structures Congress (ISSC 2018), Vol. 2 IOS Press; 2018:193-277.
20. Polinder H, Ferreira J, Jensen B, Abrahamsen A, Atallah K, McMahon R. Trends in wind turbine generator systems. *IEEE Trans Emerging Sel Topics Power Elect*. 2013;1:174-185.
21. Moghadam F, R Nejad A. Experimental Validation of Angular Velocity Measurements for Wind Turbines Drivetrain Condition Monitoring. In: ASME 2019 2nd International Offshore Wind Technical Conference 2019 Dec 13 American Society of Mechanical Engineers Digital Collection; 1-9.
22. Manwell J, McGowan J, Rogers A. *Wind Energy Explained: Theory, Design and Application*: John Wiley & Sons; 2010.
23. IEC 61400-4. Wind turbines part 4: Standard for design and specification of gearboxes; 2012.
24. Zhang Z, Matveev A, Øvrebø S, Nilssen R, Nysveen A. State of the art in generator technology for offshore wind energy conversion systems. In: IEEE International Electric Machines Drives Conference (IEMDC) IEEE; 2011:1131-1136.
25. Polinder H, Pijl A, Vilder G, Tavner PJ. Comparison of direct-drive and geared generator concepts for wind turbines. *IEEE Trans Energy Convers*. 2007;21:725-733.
26. Grauers A. Design of Direct-Driven Permanent-Magnet Generators for Wind Turbines. *Ph.D thesis*. Sweden: Chalmers University of Technology; 1996.
27. Li H, Chen Z, Polinder H. Optimization of multibrid permanent-magnet wind generator systems. *IEEE Trans Energy Conv*. 2009;24:82-92.
28. Dubois MR, Polinder H, Ferreira JA. Comparison of generator topologies for direct-drive wind turbines. In: Proc. 2000 Nordic Countries Pow. And Indust. Elec; 2000:22-26.
29. Hartviksen H. *Application of scaling laws for direct drive permanent magnet generators in wind turbines, Master thesis*. Norway: Norwegian University of Science and Technology; 2015.
30. Polinder H, Bang D, Van Rooij R, McDonald A, Mueller M, 10 MW. wind turbine direct-drive generator design with pitch or active speed stall control. *IEEE Int Elect Mach Drives Conf (IEMDC)*. 2007;2:1390-1395.
31. Nejad A, Guo Y, Gao Z, Moan T. Development of a 5MW reference gearbox for offshorewind turbines. *Wind Energy*. 2016;19:1089-1106.
32. Nejad A, Xing Y, Guo Y, Gao Z, Keller J, Moan T. Effects of floating sun gear in a wind turbine's planetary gearbox with geometrical imperfections. *Wind Energy*. 2015;18:2105-2120.
33. Nejad AR. Modelling and analysis of drivetrains in offshore wind turbines. *Offshore Wind Energy Technology*; 2018:37.
34. Voltages. IEC Standard IEC 60038; 2009.
35. Rotating electrical machines rating and performance. IEC 60034-1; 2017.
36. Langhart J, Ha T. How to get most realistic efficiency calculation for gearboxes. Power Transmission Engineering; 2015.
37. Moghadam F, Ebrahimi S, Oraee A, Velni JM. Vector control optimization of DFIGs under unbalanced conditions. *Int Trans Elect Energy Syst*. 2018;28:e2583.
38. Gieras JF. Permanent magnet motor technology: design and applications. CRC press; 2009.
39. Miliani E, Ayad MY, Depernet D, Kauffmann JM. Experimental analysis of a six phase permanent magnet synchronous generator in a variable speed constant frequency generating system. In: In APEC 07-Twenty-Second Annual IEEE Applied Power Electronics Conference and Exposition; 2007:1727-1732.
40. Gieras JF. Permanent magnet motor technology: design and applications. CRC press; 2009.
41. Hegseth JM, Bachynski EE. A semi-analytical frequency domain model for efficient design evaluation of spar floating wind turbines. *Marine Struct*. 2019;64:186-210.

42. Kato S, Inui Y, Michihira M, Tsuyoshi A. A low-cost wind generator system with a permanent magnet synchronous generator and diode rectifiers. In: Proceedings of the International Conference on Renewable Energy and Power Quality (ICREPQ'07). 2007:38-44.
43. Hung JY, Ding Z. Design of currents to reduce torque ripple in brushless permanent magnet motors. *IEE Proc B (Electric Power Appl)*. 1993;40:260-266.
44. Thomson W. Theory of vibration with applications. CRC press; 2018.
45. Nejad AR, Bachynski EE, Moan T. Effect of axial acceleration on drivetrain responses in a spar-type floating wind turbine. *ASME J Offshore Mech Arct Eng*. 2019;141:031901-031907.

How to cite this article: Moghadam FK, Nejad AR. Evaluation of PMSG-based drivetrain technologies for 10 MW floating offshore wind turbines: pros and cons in a life-cycle perspective. *Wind Energy*. 2020;1–22. https://doi.org/10.1002/we.2499